Journal of Manufacturing Engineering, ISSN: 0973-6867, December 2024, Vol. 19, Issue. 4, pp 136-145
DOI: https://doi.org/10.37255/jme.v19i4pp136-145

PARAMETRIC OPTIMIZATION OF WARM DEEP DRAWING PROCESS OF 304 STAINLESS STEEL CYLINDRICAL CUPS

*Dushyanth Chinthala, Devendar G and Chennakesava Reddy

Department of Mechanical Engineering, JNT University, Hyderabad, Telangana-500 085, India

Abstract

The present work is a comprehensive parametric optimization of the warm deep drawing process of 304 stainless steel. The warm deep drawing process is a crucial metal forming technique that leverages elevated temperatures to enhance the material's formability and reduce defect occurrence. This study systematically investigates the influence of various process parameters, including sheet thickness, temperature, coefficient of friction, and strain rate, on the quality of the final product in order. Using the Taguchi method for the design of experiments and Finite Element Analysis (FEA) for simulation, the research aims to determine the optimal settings for these parameters. Every parameter played its part in responses. All the factors had a similar impact on the cups designed. The strain-based FLDs are prepared to study the strain levels in the process. The optimized cup was the trail 8 cup with 1 mm, 300°C, 0.02 and 1000s^{-1}.

Keywords: *Sheet thickness, Coefficient of Friction, SS 304, Cylindrical cups.*

1. Introduction

Deep drawing is a sheet metal forming technique where a blank holder constrains a flat blank while the central portion is pushed into a die to create a deep, cuplike shape. There are many process parameters governing the quality of cups, and some are studied. R. Padmanabhan et al. [1] applied a combination of the Finite Element Method (FEM) and the Taguchi technique to assess the impact of critical process variables, such as die radius, blank holder force, and friction coefficient, in the deep drawing process. Ayari et al. [2] performed a parametric study on the deep drawing process using a Finite Element Method (FEM) model developed with ABAQUS/Explicit standard code. The study's experimental findings were compared with the FEM model results, highlighting the critical role of these parameters in the deep drawing process. Gowtham et al. [3] investigated the impact of varying the die radius on several parameters, including effective stress, effective strain, maximum principal stress, maximum principal strain, damage value, and the required load. Their study concluded that the die radius is a crucial design parameter. Pandhare et al. [4] utilized FE simulations to optimize the blank holder force (BHF) in the deep drawing process, focusing on the friction properties of CRDQ steel. They examined the forming limit diagram (FLD) across different friction coefficients and identified the optimal BHF value that minimizes wrinkling defects and failures. Reddy et al. [5] examined the deep drawing capability of Nickel 201 cylindrical cups. They found that punch velocity and strain rate were the primary factors affecting the process, resulting in increased effective stress at higher punch velocities. Reddy et al. [6] studied the deep drawing process of Monel 400 cylindrical cups, focusing on the influence of various process parameters. Their investigation revealed that punch velocity and displacement per step were the most significant parameters affecting the deep drawing capability of Monel 400 cups. Bhargavi et al. [7] optimized the process parameters for the cold deep drawing of Inconel 600 conical cups. They discovered that more raw materials could be drawn and formed into taller cups with thicker sheets. Nithin Sai et al. [8] conducted simulations to optimize Nickel 201 conical cups. They observed that a higher coefficient of friction resulted in a greater surface expansion ratio. These findings provide valuable guidance for optimizing the deep drawing process of Nickel 201 conical cups, allowing manufacturers to achieve desired cup characteristics by adjusting the coefficient of friction and blank thickness.

2. Material and Methodology

Stainless steel 304 is the material used to produce cylindrical deep-drawn cups. SS 304, also known as 18/8 stainless steel, is a widely used austenitic stainless-steel alloy due to its exceptional corrosion resistance, formability, and weldability. The alloy contains 18% chromium and 8% nickel, which provides superior corrosion resistance compared to other stainless-steel grades.

**Corresponding Author - E- mail: dushyanth5472@gmail.com*

Journal of Manufacturing Engineering, ISSN: 0973-6867, December 2024, Vol. 19, Issue. 4, pp 136-145
DOI: https://doi.org/10.37255/jme.v19i4pp136-145

2.1 Formulae for deep drawing cylindrical cups

The blank size is determined by equalling the finished drawn cup's surface area with the blank's area. The diameter of the blank is given by:

$D = \sqrt{(d^2 + 4dh)}$ for d/r > 20

$D = \sqrt{(d^2 + 4dh) - 0.5r}$ for 15< d/r < 20

$D = \sqrt{(d^2 + 4dh)} - r$ for 10 < d/r < 15

$D = \sqrt{(d - 2r)^2 + 4d(h - r) + 2\pi r(d - 0.7r)}$ for d/r < 0

where d is the mean diameter of the cup (mm), h is the height of the cup (mm), and r is the corner radius of the die (mm). The force for drawing relies on the yield strength of the material σy, diameter and thickness of the cup:

$$F_d = \pi dt(D/d - 0.6)\sigma_y$$

where D is the diameter of the blank before operation (mm), d is the diameter of the cup upon drawing (mm), t is the cup thickness (mm), and σ y is the yield strength of the blank material (N/mm^2).

The drawing punches' corner radius exceeds three times the blank thickness (t). However, the punch radius should not exceed one-fourth of the cup diameter for good flow and material distribution without failure.

3t < Punch Radius < d/4

For smooth flow of the material, the die edge radius is set preferably four to six times the blank thickness but not less than three times the sheet thickness because a lesser radius would stop material flow while an excess radius the pressure area is between the blank and the blank holder is decreased. The corner radius of the die is calculated from the following equation:

$$r = 0.8\sqrt{(D - d)t}$$

The drawing ratio is roughly given as:

D.R = D/d

The material flow in the drawing might produce flange thickening, and thinning of the cup's walls is normal. The space for drawing is kept bigger than the sheet thickness. This space is called die clearance.

$$c = t \pm \mu\sqrt{(10t)}$$

2.2 Finite element analysis

The deep drawing simulation was run using DE FORM 3D software. The top and bottom die are calculated per the formula and modelled in the software. The blank(workpiece) is made with the diameter D from eq. (1) and is meshed with tetrahedral elements. The corner radii are changed for every thickness, and so is the slight variation in the die's radius. Every combination in the L9 array is simulated, and results are extracted from the software's post-processing window. Figures 1 and 2 show the Finite element model of the sheet metal and die.

The number of elements in the blank: 7089

The number of nodes in the blank: 2382

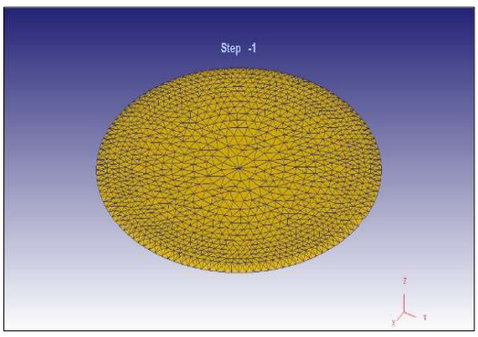

Figure 1 Meshed sheet metal

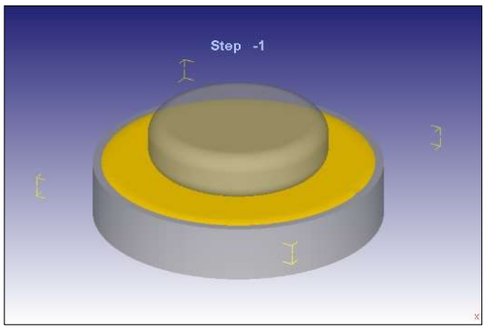

Figure 2 Die and sheet metal as a couple

Journal of Manufacturing Engineering, ISSN: 0973-6867, December 2024, Vol. 19, Issue. 4, pp 136-145
DOI: https://doi.org/10.37255/jme.v19i4pp136-145

Table 1 Process parameters and levels

Factors		Level 1	Level 2	Level 3
Thickness (mm)	A	0.5	0.75	1
Temperature (°C)	B	100	300	500
Coefficient of friction (μ)	C	0.02	0.04	0.08
Strain rate (s^{-1})	D	100.00	500.00	1000.00

Table 2 L9 Orthogonal Array

Trial	A	B	C	D
1	0.5	100	0.02	100
2	0.5	300	0.04	500
3	0.5	500	0.08	1000
4	0.75	100	0.04	1000
5	0.75	300	0.08	100
6	0.75	500	0.02	1000
7	1	100	0.08	500
8	1	300	0.02	1000
9	1	500	0.04	100

Table 3 ANOVA table with Effective Stress as a response

Factor	S1	S2	S3	SS	v	V	F	P
A	313.30	294.30	289.94	102.85	1	102.85	8570.83	6.96
B	346.00	295.28	256.26	1349.82	1	1349.82	112485.00	91.36
C	294.98	298.46	304.10	14.12	1	14.12	1176.67	0.96
D	297.26	296.50	303.78	10.67	1	10.67	889.17	0.72
e				0.01	4	0.00	0.00	0.00
T	1251.54	1184.54	1154.08	1477.47	8			100.00

3. Results

3.1 Influence of factors on effective stress

The process parameters considered for the study are listed in Table 1, along with their respective levels. The experimental design was structured using the L9 orthogonal array, as shown in Table 2. Table 3 is tabulated using the ANOVA statistic technique and the appropriate formula. The Fisher's test column ascertains the parameters (A, B, C, and D) accepted at a 90% confidence level for the variation. The percentage contribution shows that the thickness of the sheet contributes to 6.96% of the variation, and the coefficient of friction strain rate held no significance. The contribution of temperature is 91.36%. SS is the sum of squares, v is the degrees of freedom, V is the variance, F is the Fisher's ratio, P is the contribution percentage, and T is the sum of squares due to total variation.

There is a larger effect of temperature on the effective stress, evident from the ANOVA table with the highest contribution of 91%, and there is a small effect of other thicknesses on the effective stress. The other 2 factors have no impact on the effective stress.

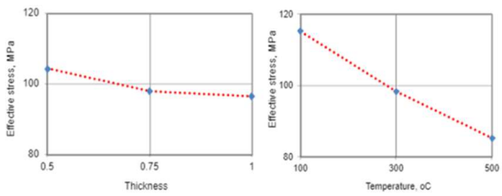

Figure 3 Variation of parameters with Effective stress

Journal of Manufacturing Engineering, ISSN: 0973-6867, December 2024, Vol. 19, Issue. 4, pp 136-145
DOI: https://doi.org/10.37255/jme.v19i4pp136-145

Figure 3 illustrates the relationship between process parameters and the effective stress observed during the experiments. There is a sharp decrease in effective stress with increasing temperature. It is evident that with increased temperature, the stress produced decreases, and the load required to deform into cups decreases. The temperature increase resulted in improved formability of sheet metal. Also, the thickness of the material, which is not a significant factor with a low percentage of contribution, but the lower thickness, which is 0.5 mm, had more effective stress-induced, but there is not much of a change when the thickness is 1 mm and upwards.

3.2 Sample and procedure

The ANOVA test for the cup's effective strain is given in Table 3. The Fisher's test column ascertains the parameters (A, B, C, and D) accepted at a 90% confidence level for the variation. The percentage contribution shows that the thickness of the sheet contributes to 65.09% of the variation, the coefficient of friction contributes to 10.58% of the variation, and the strain rate holds 24.08% of the variation. The contribution of temperature is negligible. There is some peculiarity visible in the graph trends slightly increasing at low thickness and decreasing at higher thicknesses. All the parameters studied do not follow the conventional trend; at lower thicknesses, the deformation is an easy metal flow. At lower thickness, the blank adapts to the load and quickly deforms into a shape with less strain. However, the blank resists deformation at a slightly higher thickness, resulting in more effective strain. The material is much more resistant at the highest thickness, and strain doesn't exceed the limit. The effective strain was found to be high for μ=0.04 and less at remaining levels. The strain rate 500s^(-1) was attributed to the highest strain, while the fast and slow deformation maintained low strain. Figure 4 depicts the effective stress distribution across the cups obtained during the experiments.

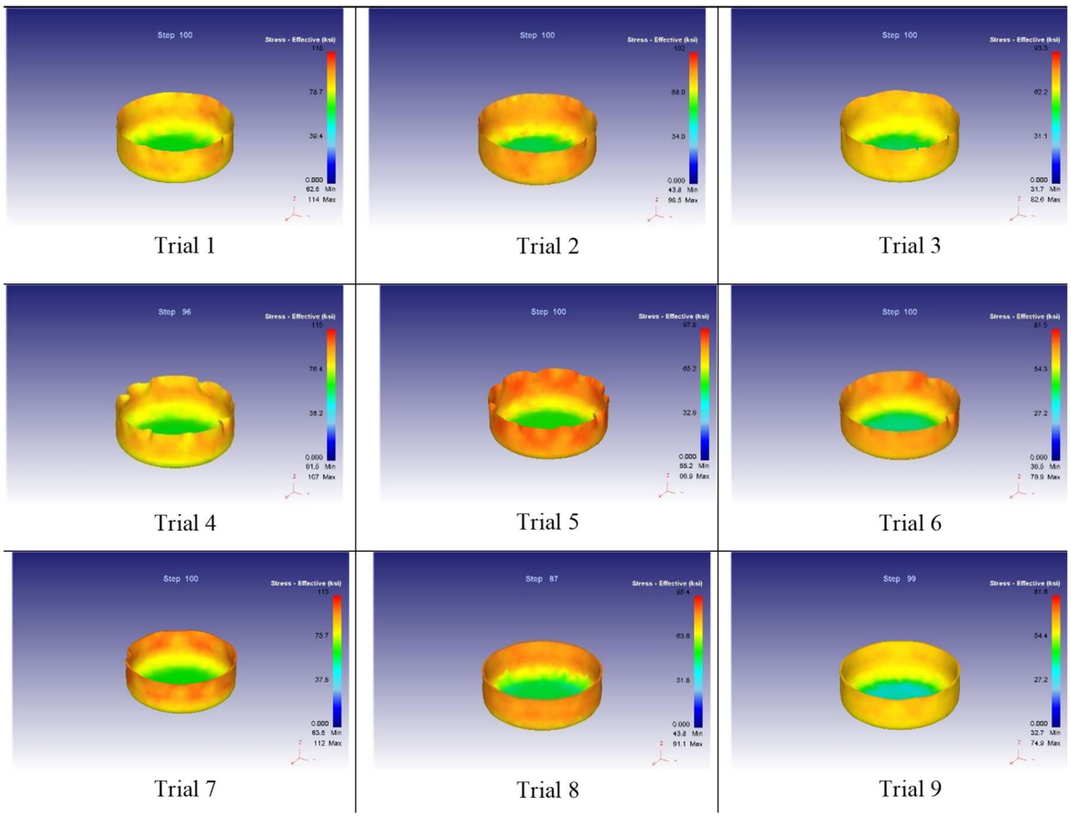

Figure 4 Effective stress of cups

Journal of Manufacturing Engineering, ISSN: 0973-6867, December 2024, Vol. 19, Issue. 4, pp 136-145
DOI: https://doi.org/10.37255/jme.v19i4pp136-145

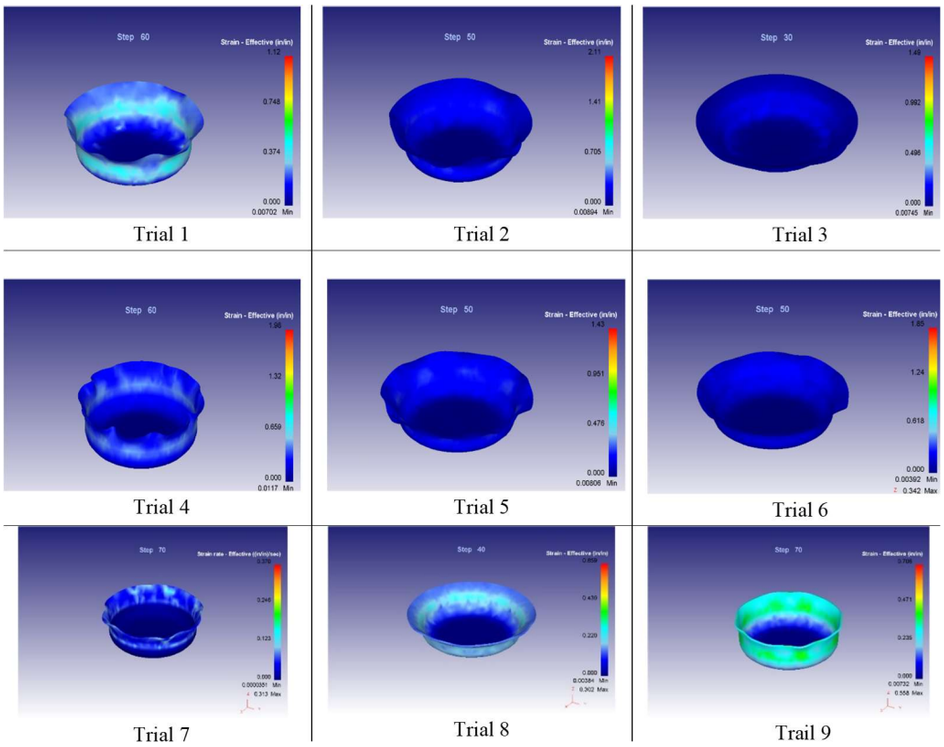

Figure 5 Effective strain of cups

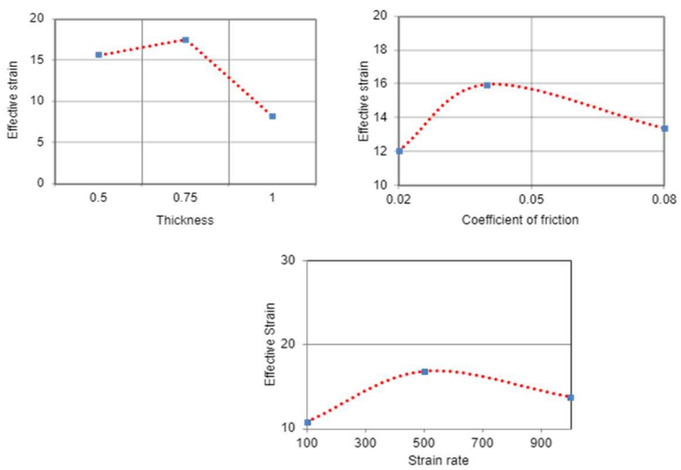

Figure 6 Variation of factors with effective strain

Figure 5 presents the effective strain distribution in the cups produced during the experiments. Figure 6 illustrates the influence of various factors on the effective strain.

Journal of Manufacturing Engineering, ISSN: 0973-6867, December 2024, Vol. 19, Issue. 4, pp 136-145
DOI: https://doi.org/10.37255/jme.v19i4pp136-145

Table 4 ANOVA table for Surface expansion ratio as a response

Factor	S1	S2	S3	SS	v	V	F	P
A	34	36.3	36	1.04	1	1.04	52.00	26.46
B	33.7	36	36.6	1.56	1	1.56	78.00	39.69
C	34.5	35.9	35.9	0.43	1	0.43	21.50	10.94
D	34.1	36.1	36.1	0.88	1	0.88	44.00	22.39
e				0.02	4	0	0.00	0.52
T	136.3	144.3	144.6	3.93	8			100

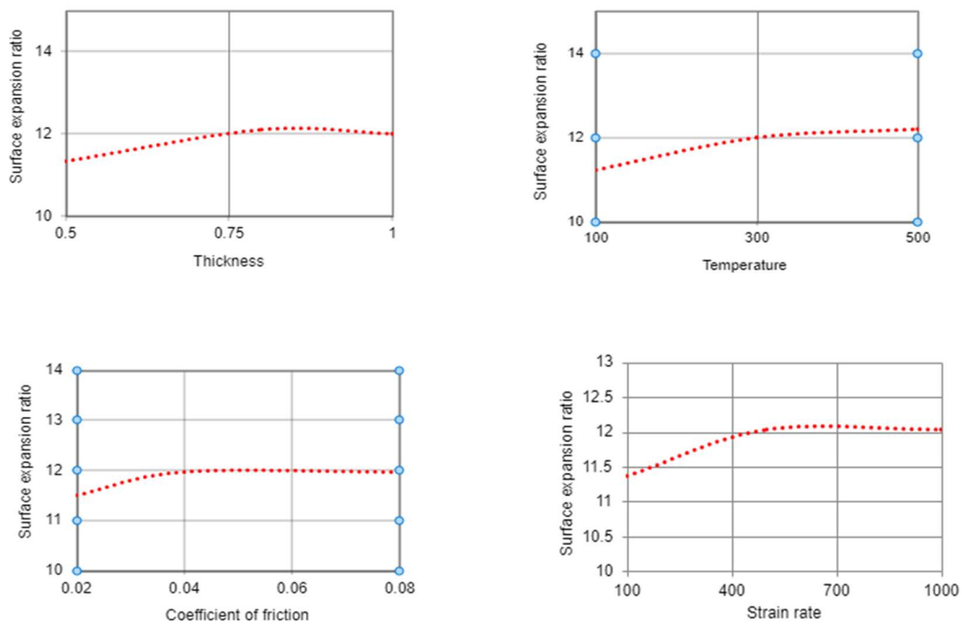

Figure 7 Variation of factors with a Surface expansion ratio

3.3 Influence of Factors on Surface expansion ratio of the cup

Figure 7 shows the variation of factors with a Surface expansion ratio. Analysis of Variance (ANOVA) was conducted to evaluate the influence of process parameters on the surface expansion ratio, as shown in Table 4. The ANOVA summary of cup damage is given in the table. The Fisher's test column ascertains all the parameters (A, B, C, and D) accepted at a 90% confidence level influencing the variation. The percentage contribution indicates that the thickness of the sheet gives 26.46% of the variation, the coefficient of friction contributes 10.94%, and the strain rate controls 22.39% of the variation. The influence of temperature is 39.69%.

There is an increase in the surface expansion ratio with increasing thickness, and the surface expansion ratio increases with increasing temperature in the above graph. The temperature of the blank and heat transfer between the dies plays a role in the surface expansion. The higher the thickness, the more resistance to surface expansion. The coefficient of friction is also proportional to the surface expansion. Fast deformation results in more expansion, and steady deformation keeps the material uniform, resulting in less surface expansion.

3.4 Influence of Factors on Damage of the Cup

The ANOVA summary of cup damage is given in Table 5. The Fisher's test column ascertains all the

Journal of Manufacturing Engineering, ISSN: 0973-6867, December 2024, Vol. 19, Issue. 4, pp 136-145
DOI: https://doi.org/10.37255/jme.v19i4pp136-145

parameters (A, B, C, and D) accepted at a 90% confidence level influencing the variation. The percentage contribution indicates that the thickness of the sheet gives 63.54% of the variation, the coefficient of friction contributes 2.99%, and the strain rate controls 46.63% of the variation. The influence of temperature is 16.2%.

The damage decreases with increasing thickness, suggesting larger thicknesses' susceptibility to the damage produced. Quick deformation shows more damage to the cups than the slowly controlled deformations; a lower strain rate helps control the damage. The damage decreases and increases within three temperatures, which is credited to the heat transfer between the dies and the blank sheet. The die temperature was set near 300°C. Hence, the damage is low at this temperature. Figure 8 shows the Surface expansion ratios of the cups in Finite element analysis. Figure 9 shows the variation of process parameters with damage. Figure 10 illustrates the damage of the cups.

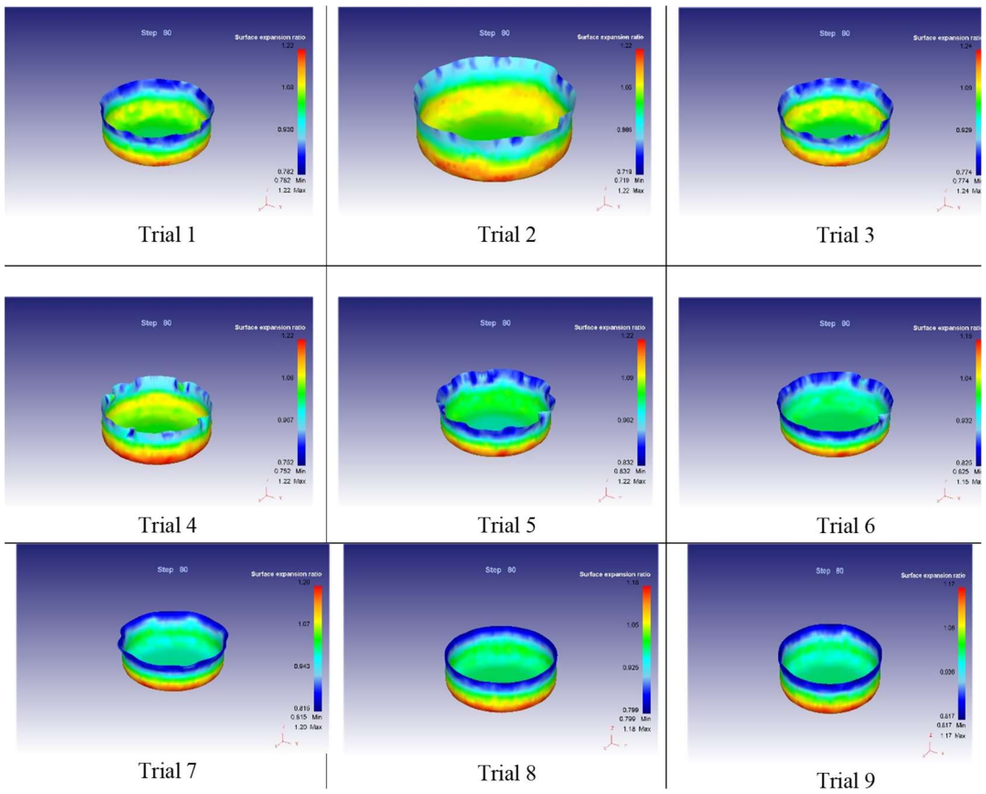

Figure 8 Surface expansion ratios of the cups

Table 5 ANOVA table for Damage as a response

Factor	S1	S2	S3	SS	v	V	F	P
A	4.177	2.314	1.216	1.49	1	1.49	99.43	63.54
B	2.952	1.691	3.064	0.38	1	0.38	25.36	16.2
C	2.448	2.327	2.932	0.07	1	0.07	4.67	2.99
D	2.27	1.993	3.444	0.39	1	0.39	26.03	16.63
e				0.014985	4	0	0.00	0.64
T	11.847	8.325	10.656	2.344985	8			100

Journal of Manufacturing Engineering, ISSN: 0973-6867, December 2024, Vol. 19, Issue. 4, pp 136-145
DOI: https://doi.org/10.37255/jme.v19i4pp136-145

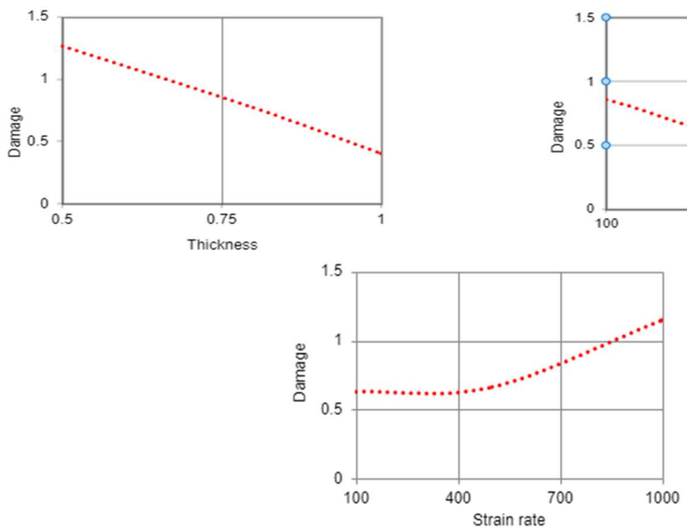

Figure 9 Variation of process parameters with damage

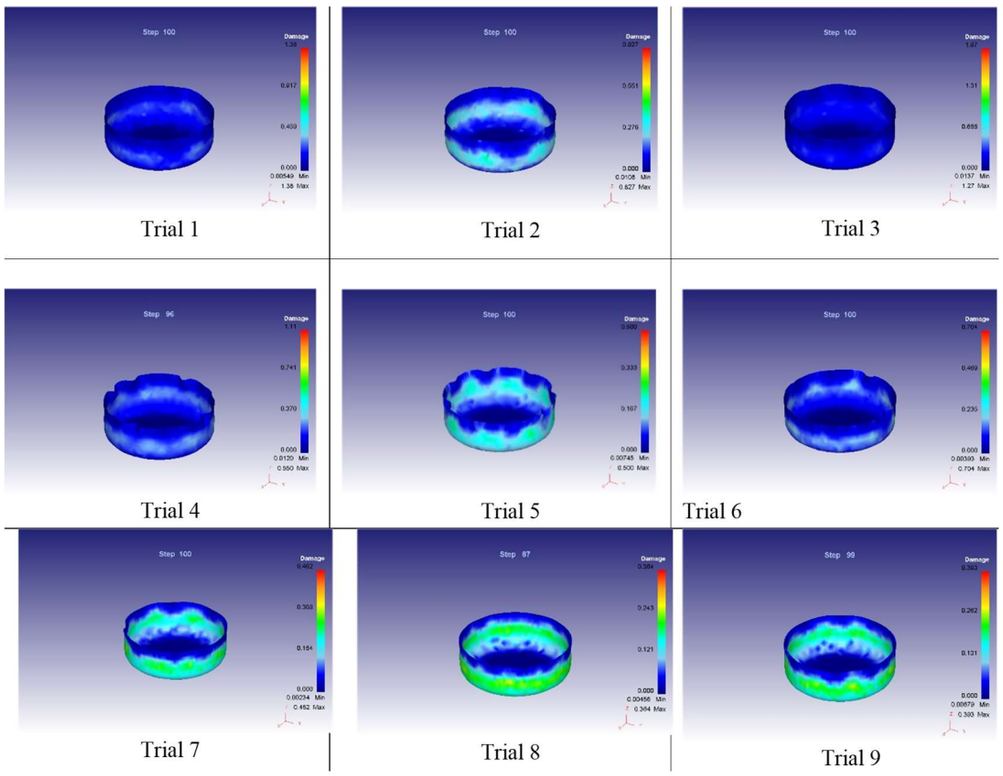

Figure 10 Damage of the cups

Journal of Manufacturing Engineering, ISSN: 0973-6867, December 2024, Vol. 19, Issue. 4, pp 136-145
DOI: https://doi.org/10.37255/jme.v19i4pp136-145

3.5 Formability limit diagram

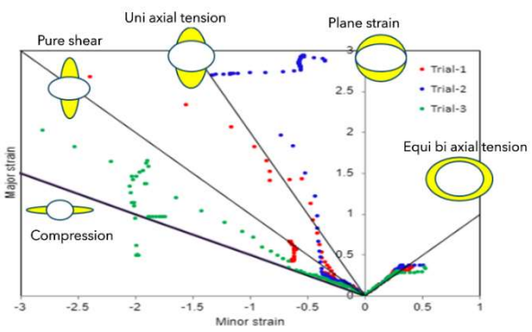

Figure 11(a) FLD of trails 1, 2 & 3 with 0.5mm thickness

Figure 11 shows the formability limiting diagrams. The diagram has some elements having strains beyond the desired limit, that is, at the compression region of the curve and also many point scatterings at the top of the diagram, which are responsible for the wrinkling and defects in trials 1,2, and 3. All three had strain points beyond the limit, leading to some damage in the cups.

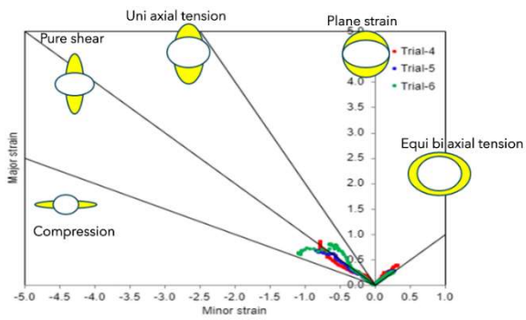

Figure 11(b) FLD of trials 4, 5 & 6 with 0.75 mm thickness

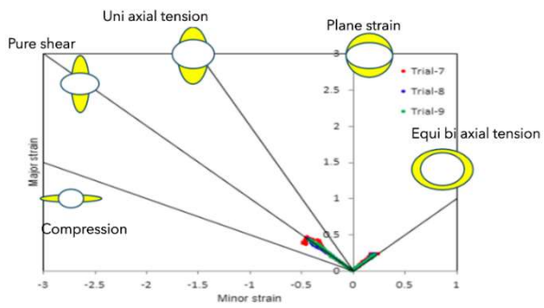

Figure 11(c) FLD of trials 7, 8 & 9 with 1 mm thickness

The strain levels of the FLD of trials 4,5&6 and have a cluster of the strain value points in the diagram, which pertains to less damage and wrinkles than in the first trials. However, some tendency towards compression and non-linearity in the points resulted in slight damage and wrinkles in the cups. This diagram has a solid cluster without much variation in the strain points. The strain values are within the limit of forming and are better than the previous FLD diagrams.

3.6 Fabrication of Deep drawn cups

Figure 12 illustrates the deep drawing machine with a hydraulic-powered press. The deep-drawn cups are made using a deep-drawing machine with a hydraulic-powered press. The blanks are cut to the calculated diameter and are heated to the required temperature. The heated blank is safely put above the die cavity, and the hydraulic press is applied to get the cups. They are removed and placed aside to cool down.

Figure 12 Deep drawing machine with hydraulic-powered press

The lever is used to advance the press towards blank material and die and also withdrawn when the shape of the cup assumes the shape of the die completely. After the drawing, the cup is removed from the die cavity using the tongs. Figure 13 shows the photograph of the cup in the experimental trial 8.

Journal of Manufacturing Engineering, ISSN: 0973-6867, December 2024, Vol. 19, Issue. 4, pp 136-145
DOI: https://doi.org/10.37255/jme.v19i4pp136-145

Figure 13 Trail 8-cup

4. Conclusion

Various factors, including temperature, thickness, coefficient of friction, and strain rate, influence sheet metal's performance during forming processes. Increased temperature leads to a decrease in the effective stress of the sheet metal while the surface expansion ratio increases. Interestingly, damage initially decreases with increasing temperature but then starts to increase again. The thickness of the sheet metal also plays a role, with thinner materials (0.5 mm) experiencing more effective stress than thicker ones. The effective strain shows a notable value at 0.5 mm thickness, but not much change is observed for thicknesses of 1 mm and above. The surface expansion ratio increases with increasing thickness, and damage is inversely proportional to thickness, meaning thicker materials tend to have less damage. The coefficient of friction also affects the forming process, with the effective strain fluctuating as the coefficient changes. The surface expansion ratio is less at low friction coefficients and remains steady at higher coefficients. Finally, the strain rate has a significant impact, with effective strain increasing and then decreasing as the strain rate increases, while damage consistently increases with higher strain rates. Understanding the interplay of these factors is crucial for optimizing sheet metal forming processes and ensuring the desired performance of the final product. The optimal cup found within the process parameters with little damage is found to be the cup of trial number 8 with factors 1 mm, 300℃, 0.02 and 1000 s^{-1}.

References

1. *R., Padmanabhan & Oliveira, M. & Alves, J.L. & Menezes, L. (2007). Influence of process parameters on the deep drawing of stainless steel. Finite Elements in Analysis and Design. Finite Elements in Analysis and Design Vol.43, Issue.14, pp:1062 -106.*

2. *F, Ayari & Lazghab, Tarek & Bayraktar, Emin. (2009). Parametric Finite Element Analysis of Square cup deep drawing. Computational Material Science and Surface Engineering Vol.1, Issue 2, pp:106 - 111*

3. *Gowtham, Kopanathi & Srikanth, K.V.N.S. & Murty, K.L.N. (2012). Simulation of The Effect of Die Radius on Deep Drawing Process. International Journal of Applied Research In Mechanical Engineering (IJARME) Issn: 2231 5950, Volume 2, Issue 1.*

4. *G. Devendar, A. C. Reddy (2016) Formability Limit Diagrams of Cold Deep Drawing Process for Nickel 201 Cylindrical Cups. International Journal of Science and Research (IJSR) Volume 5 Issue 8.*

5. *G. Devendar, A. C. Reddy (2021) Parametric Optimization of Monel 400 Cold Deep Drawn Cylindrical Cups, International Journal of Materials Science ISSN 0973 4589 Volume 16, Number 1, pp. 17 -31.*

6. *K. Bargavi, G. Devendar, A. C. Reddy (2020) Optimization of Process Parameters of Deep Drawing Process for Inconel 600 Conical Cups, International Journal of Materials Science ISSN 0973 4589 Volume 15, Number 2, pp. 97 - 109.*

7. *J. Nithin Sai, G. Devendar, A. C. Reddy (2020) Parametric Optimization of NI201 Deep Drawn Conical Cups, International Journal of Material Sciences and Technology. ISSN 2249 3077 Volume 10, Number 2 (2020), pp. 81- 93.*

8. *A.C. Reddy, Homogenization and Parametric Consequence of Warm Deep Drawing Process for 1050A Aluminium Alloy: Validation through FEA, International Journal of Science and Research, vol. 4, no. 4, pp. 2034-2042, 2015.*

9. *A. C. Reddy, Performance of Warm Deep Drawing Process for AA1050 Cylindrical Cups with and Without Blank Holding Force, International Journal of Scientific Research, vol. 4, no. 10, pp. 358-365, 2015.*